scientific reports

Check for updates

OPEN

GLUT1 overexpression enhances glucose metabolism and promotes neonatal heart regeneration

Viviana M. Fajardo[1], Iris Feng[2], Bao Ying Chen[3,5], Cesar A. Perez-Ramirez[4], Baochen Shi[2], Peter Clark[3,5], Rong Tian[6], Ching-Ling Lien[7,8,9], Matteo Pellegrini[2,11,12], Heather Christofk[4,11,12], Haruko Nakano[2] & Atsushi Nakano[2,10,11,12,13]✉

The mammalian heart switches its main metabolic substrate from glucose to fatty acids shortly after birth. This metabolic switch coincides with the loss of regenerative capacity in the heart. However, it is unknown whether glucose metabolism regulates heart regeneration. Here, we report that glucose metabolism is a determinant of regenerative capacity in the neonatal mammalian heart. Cardiac-specific overexpression of Glut1, the embryonic form of constitutively active glucose transporter, resulted in an increase in glucose uptake and concomitant accumulation of glycogen storage in postnatal heart. Upon cryoinjury, Glut1 transgenic hearts showed higher regenerative capacity with less fibrosis than non-transgenic control hearts. Interestingly, flow cytometry analysis revealed two distinct populations of ventricular cardiomyocytes: Tnnt2-high and Tnnt2-low cardiomyocytes, the latter of which showed significantly higher mitotic activity in response to high intracellular glucose in Glut1 transgenic hearts. Metabolic profiling shows that Glut1-transgenic hearts have a significant increase in the glucose metabolites including nucleotides upon injury. Inhibition of the nucleotide biosynthesis abrogated the regenerative advantage of high intra-cardiomyocyte glucose level, suggesting that the glucose enhances the cardiomyocyte regeneration through the supply of nucleotides. Our data suggest that the increase in glucose metabolism promotes cardiac regeneration in neonatal mouse heart.

Heart disease is the leading cause of death worldwide. This is in part due to the fact that the heart is the least regenerative of organs in the body. As a result, the loss of cardiomyocytes is compensated by the increase in the workload of the remaining cardiomyocytes. However, recent studies revealed that postnatal cardiomyocytes can renew at a very low but measurable rate. Neonatal mouse heart can fully regenerate up to 15% of the muscle during the first 7 days of life[1]. In human heart, cytokinesis of cardiomyocytes is detected until up to 20 years old resulting in a 3.4-fold increase in the number of cardiomyocytes since birth[2]. Pulse-chase study of atmospheric ^{14}C from nuclear weapon tests suggests that human adult cardiomyocytes also undergo cytokinesis and its turnover rate is calculated to be 1% per year at age 25, declining to 0.45% by the age of 75[3,4]. These observations can potentially be therapeutically exploited[5]. The mitotic activity of mammalian cardiomyocytes during the fetal stages is rapidly lost shortly after birth, a process known as terminal differentiation[6]. Rapid conversion from hyperplastic growth to hypertrophic enlargement at this stage coincides with the polyploidization. In rodents, the

[1]Division of Neonatology, Department of Pediatrics, David Geffen School of Medicine, University of California Los Angeles, Los Angeles, CA, USA. [2]Department of Molecular, Cell, Developmental Biology, School of Life Science, University of California Los Angeles, Los Angeles, CA, USA. [3]Department of Molecular and Medical Pharmacology, University of California, Los Angeles, Los Angeles, CA, USA. [4]Department of Biological Chemistry, David Geffen School of Medicine, University of California Los Angeles, Los Angeles, CA, USA. [5]Crump Institute for Molecular Imaging, University of California Los Angeles, Los Angeles, CA, USA. [6]Department of Anesthesiology and Pain Medicine, University of Washington, Seattle, WA, USA. [7]The Saban Research Institute of Children's Hospital Los Angeles, Los Angeles, CA, USA. [8]Department of Surgery, University of Southern California, Los Angeles, CA, USA. [9]Department of Biochemistry and Molecular Biology, Keck School of Medicine, University of Southern California, Los Angeles, CA, USA. [10]Division of Cardiology, Department of Medicine, University of California Los Angeles, Los Angeles, CA, USA. [11]Molecular Biology Institute, University of California Los Angeles, Los Angeles, CA, USA. [12]Eli and Edythe Broad Center of Regenerative Medicine and Stem Cell Research, University of California Los Angeles, Los Angeles, CA, USA. [13]Department of Cell Physiology, The Jikei University School of Medicine, Tokyo, Japan. ✉email: anakano@ucla.edu

polyploidization usually accompanies karyokinesis (nuclear division) without cytokinesis (cell division). Remaining mononucleated myocytes may be responsible for postnatal proliferation of murine myocytes[1,7,8]. Not only the nuclear dynamics, but the response to extracellular signals also changes before and after terminal differentiation.

Interestingly, the loss of cardiac regenerative capacity coincides with the metabolic switch of energy source. The heart consumes the most energy per gram of tissue in the body, and the cardiac muscle develops a unique structure and biochemical machinery to meet its high energy demand[9]. The embryonic heart depends mainly on glucose for ATP production, while in adult heart more than 95% of cardiac ATP is generated from fatty acid oxidation. However, during physiological embryogenesis in mice, cardiac glucose uptake drastically decreases from E10.5. This timing is long before the metabolic switch from glucose to fatty acid after birth. We have previously found that the anabolic biosynthesis of building blocks from glucose, but not the catabolic extraction of energy, is a key regulator of cardiac maturation during late embryogenesis, raising an intriguing possibility that glucose is not merely to meet the energy demand but to regulate the genetic program of cardiac maturation[10].

While recent studies have found that glucose level regulates cardiogenesis, little is known about whether and how glucose impacts the regenerative capacity of the heart in vivo. In this study, we report that an increase in the glucose metabolism in αMHC-hGLUT1 transgenic mice potentiates the regenerative capacity and inhibits fibrosis upon neonatal heart injury. Interestingly, we found two distinct populations of cardiomyocytes: Tnnt2^{high} and relatively immature Tnnt2^{low} cardiomyocytes. Tnnt2^{low} cardiomyocytes display a three- to four-fold increase in mitotic activity and twofold increase in number in response to the increase metabolism. Glucose metabolites are significantly increased in injured Glut1 transgenic hearts, and the regenerative advantage of Glut1 transgenic hearts was abrogated by inhibition of the nucleotide biosynthesis pathway, suggesting that glucose promotes cardiac regeneration through the supply of nucleotides. Together, our results demonstrate that glucose metabolism is a determinant of regenerative capacity in neonatal mammalian heart.

Results

Glut1 transgenic hearts show higher glucose uptake at the basal level. Glucose is among the most tightly regulated nutrients. To increase the intra-cardiomyocyte glucose metabolism, we used α*MHC-hGLUT1* transgenic mouse line[11]. This mouse line overexpresses human GLUT1 in a cardiac-specific manner. Glut1 is an insulin-independent constitutively active glucose transporter expressed in the embryonic heart. In the postnatal heart, glucose transport is regulated predominantly by insulin-dependent Glut4 except that Glut1 becomes re-expressed in the heart upon hypertrophic stresses[12–14]. Although Glut1 is subject to heavy post-translational regulation, immunostaining and qPCR assay indicate that GLUT1 transgene is expressed strongly in the cardiac cytoplasm and sarcolemma in this mouse line. Upon injury, the Glut1 transgene becomes localized predominantly to the sarcolemma (Supplementary Fig. 1a,b). Autoradiographic imaging and quantification of ^{18}F-FDG-injected mouse heart suggest that ^{18}F-FDG accumulation is increased by 2.6-fold in Glut1 transgenic hearts (Glut1 tg) at P2 (Supplementary Fig. 1c,d). The ^{18}F-FDG accumulation drops after P4 possibly due to the increase in the intracardiomyocyte glucose level. Consistent with the original report[11], Glut1 transgenic mice and their wild-type (WT) control litters showed no significant difference in the body weight and heart weight (Fig. 1a and Supplementary Fig. 1f). Glut1 transgenic pups had normal but slightly lower glucose level when compared to WT at P1. However, no statistical difference was observed at P3 and P7 stages (Supplementary Fig. 1e). Thus, α*MHC-hGLUT1* transgenic mice are suitable for analyzing the effect of increased glucose uptake in the heart.

Glut1 transgenic hearts are more regenerative after injury. To test whether intra-cardiomyocyte glucose metabolism impacts the heart repair, Glut1 transgenic hearts were cryoinjured at P1 as described[15,16]. While there was no difference in the heart weight/body weight (HW/BW) ratio between WT and Glut1 transgenic hearts without injury or with sham surgery (Fig. 1a, b, and Supplementary Fig. 1f), Glut1 transgenic hearts showed a statistically significant increase in the HW/BW 7 and 14 days post-injury when compared to WT hearts (Fig. 1c,d; 7.8 ± 0.33 vs 6.7 ± 0.27 and 7.9 ± 0.24 vs 6.8 ± 0.22 at postnatal day 7 and 14, respectively, $p < 0.05$). Glut1 transgenic hearts continued to show a trend of higher HW/BW at day 21 but no statistically significant differences were seen by day 40 post-injury. To examine the fibrosis post-injury, the collagen deposition level was analyzed by H&E and Picrosirius Red stainings[17]. Image-J Software quantification of scar area/left ventricular area showed 4–5% fibrotic area in both WT and Glut1 transgenic hearts at day 7 and 14 post-injury. Cryoinjury induced up to 8–10% fibrotic area in WT hearts at P21 and P40, whereas Glut1 transgenic hearts showed a significantly lower level of fibrosis (Fig. 1e,f; 10.2 ± 1.2 vs 5.6 ± 0.85, $p < 0.01$, at P21). To determine whether the decreased level of fibrosis was associated with proliferation of cardiomyocytes in Glut1 transgenic hearts, the WT and Glut1 transgenic hearts were immunostained for PCNA (mitosis marker) and Tnnt2 (cardiac marker). Glut1 transgenic hearts showed an increase in the number of PCNA-positive cardiomyocytes (Fig. 1g and Supplementary Fig. 1g). Cardiomyocyte proliferation and angiogenesis are both required for complete regeneration of the neonatal heart after injury[18]. Vascularity tends to be increased in Glut1 transgenic heart upon injury in our study, but this is likely secondary to the cardiomyocyte proliferation as Glut1 is overexpressed specifically in cardiomyocytes (Supplementary Fig. 3). Echocardiographic analysis revealed no difference in the cardiac function between WT and Glut1 transgenic heart at P21 and 40 (Supplementary Fig. 2). Together, these data suggest that Glut1 transgenic hearts show higher regenerative capacity possibly due to the increased mitotic activity of cardiomyocytes.

Two distinct cardiomyocyte populations in neonatal hearts. As higher mitotic activity of fetal/neonatal cardiomyocytes often accompanies lower maturation level during cardiogenesis[10], we characterized the maturity of cardiomyocytes by Tnnt2 expression (a cardiac specific contractile protein) and Mitotracker (a

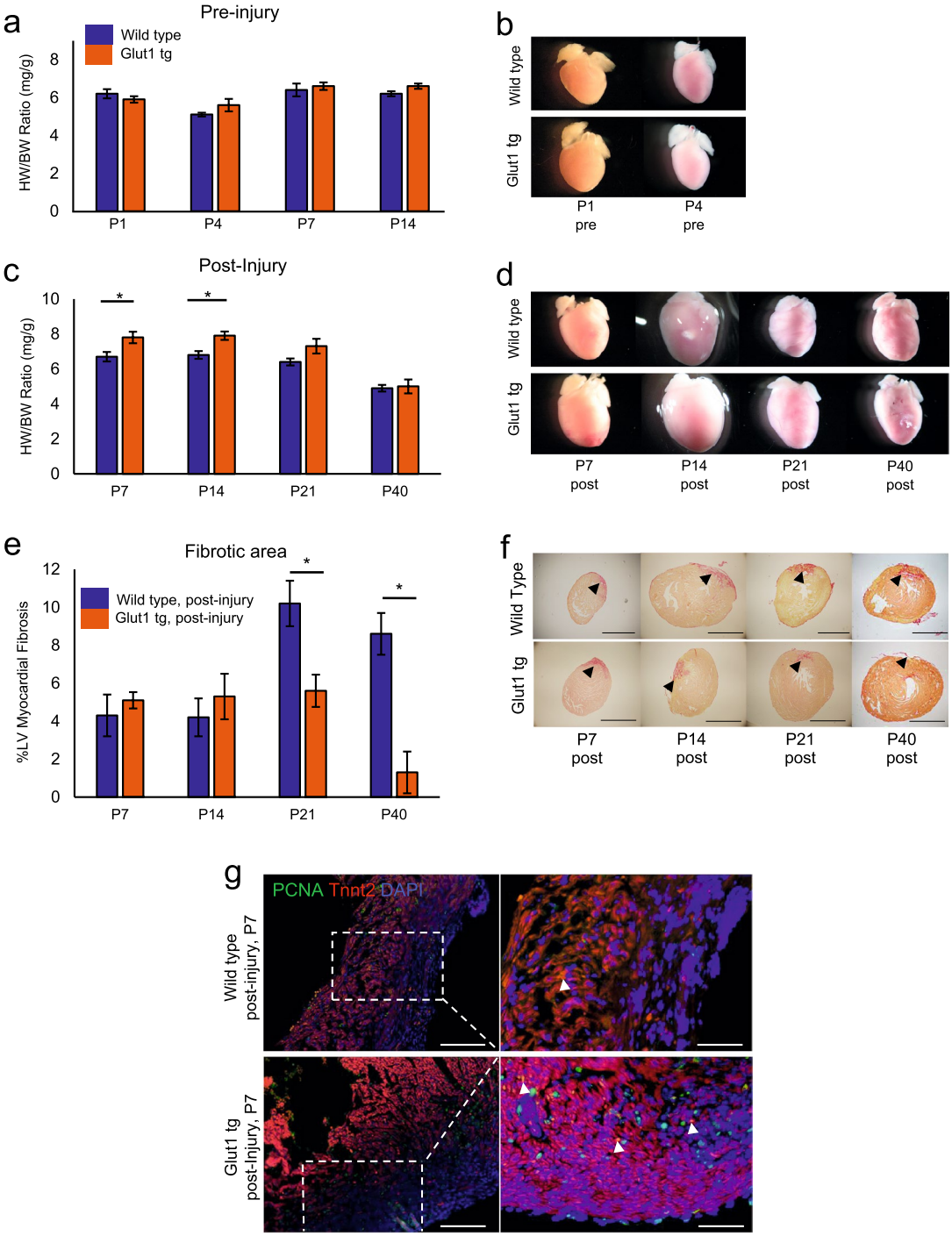

Figure 1. Increase in intracellular glucose promotes cardiac regeneration in Glut1 transgenic heart. (**a**) Heart weight-body weight (HW/BW) ratio of Wild type and Glut1 transgenic (Glut1 tg) mice without injury. n = 3–7 for each group, p = n.s. (**b**) Representative images of hearts. (**c**) Heart weight-body weight (HW/BW) ratio of Wild type and Glut1 transgenic mouse post-injury. The hearts were cryoinjured at P1 and examined at P7, 14, 21 and 40. Note that the HW/BW is higher in Glut1 transgenic hearts at P7 and 14. n = 4–9 for each group, $^*p < 0.05$. (**d**) Images of representative hearts post-injury. Note the ballooning of the heart at P14 in both wild type and Glut1 transgenic hearts. (**e**) %Fibrotic area measured by Image J capture of Picrosirius red stainings of the hearts. Hearts were cryoinjured at P1 and examined at P7, 14, 21 and 40. n = 5–8 for each group, $^*p < 0.05$. (**f**) Representative images of Picrosirius red staining of wild type and Glut1 transgenic hearts. Arrowheads indicate fibrotic area. Scale bar = 200 µm. (**g**) PCNA staining of the sections from wild type and Glut1 transgenic hearts 7 days post-injury. Sections were stained with a cardiac marker (Tnnt2; Red), proliferation marker (PCNA; Green) and a nuclear marker (DAPI; Blue). Note that PCNA staining is more abundant in Glut1 transgenic heart. Arrowheads indicate PCNA positive cardiomyocytes. Scale bar = 50 µm and 20 µm respectively.

marker of mitochondrial content). Flow cytometric analysis revealed two distinct populations of cardiomyocytes in neonatal hearts; Tnnt2^{high} and Tnnt2^{low} cardiomyocytes (Fig. 2a). Tnnt2^{high} and Tnnt2^{low} cardiomyocytes were Mitotracker^{low} and Mitotracker^{high}, respectively. As the Mitotracker does not necessarily reflect the mitochondrial function[19–21], we examined the mRNA expression signature of Tnnt2^{high} and Tnnt2^{low} cardiomyocytes genome-wide. To collect the cells alive, two populations were sorted from α*MHC-Cre^{tg}; R26$^{+/YFP\ reporter}$* hearts in both WT and Glut1 transgenic background using YFP reporter and Mitotracker (Fig. 2b). Forward scatter plot suggests that Tnnt2^{low} (Mitotracker^{high}) cardiomyocytes are slightly smaller in size (Supplementary Fig. 4c). RNA-seq analysis confirmed that Tnnt2^{low} (Mitotracker^{high}) cardiomyocytes do express a slightly lower level of Tnnt2 mRNA as compared to Tnnt2^{high} (Mitotracker^{low}) cardiomyocytes. Although Mitotracker staining level is high, mitochondrial gene expression level was lower in Tnnt2^{low} (Mitotracker^{high}) cardiomyocytes than Tnnt2^{high} (Mitotracker^{low}) cardiomyocytes in WT heart, suggesting that Tnnt2^{low} (Mitotracker^{high}) cardiomyocytes represent relatively immature cardiomyocytes and that Mitotracker does not reflect the functional maturity of mitochondria in this context, consistent with previous observations[19–21].

To examine how the increase in intra-cardiomyocyte glucose uptake impacts the expression signature of Tnnt2^{high} and Tnnt2^{low} cardiomyocytes, the RNA-seq was performed in these cell populations from WT and in Glut1 transgenic hearts. Comparison of 4 populations (Tnnt2^{high} and Tnnt2^{low} cardiomyocytes from WT and Glut1 hearts) showed only marginal differences at transcriptome level (Fig. 2c). Interestingly, however, pathway analysis revealed that Tnnt2^{low} cardiomyocytes from Glut1 transgenic heart (G1 Tnnt2^{low}) are unique in that they are enriched for the genes associated with mitosis, cell cycle, and cell division compared to the other 3 populations in WT and Glut1 transgenic hearts (Fig. 2c). Indeed, 2-way comparison between G1 Tnnt2^{low} and G1 Tnnt2^{high} cardiomyocytes identified considerably more differentially expressed genes than any 2 comparisons (918 and 349 genes up/down-regulated in G1 Tnnt2^{low} cells; Supplementary Fig. 4a). Compared to G1 Tnnt2^{high} cardiomyocytes, G1 Tnnt2^{low} cardiomyocytes are, again, enriched for the genes associated with cell cycle, cell division, and mitotic nuclear division, while cardiac genes and mitochondrial genes are expressed at a lower level (Fig. 2d,e). Together, we found two distinct populations of cardiomyocytes in neonatal heart: Tnnt2^{high} cardiomyocytes are larger, less mitotic and more mature than Tnnt2^{low} cells. On the other hand, Tnnt2^{low} cells are smaller, show less mature expression signature and upregulate cell cycle gene expression in Glut1 transgenic background.

Tnnt2-low cardiomyocytes are glucose-responders. As the cell cycle genes are upregulated only in Tnnt2^{low} cardiomyocytes upon the increase in glucose uptake in Glut1 transgenic hearts, the mitotic activity of Tnnt2^{high} and Tnnt2^{low} cardiomyocytes were measured by EdU incorporation assay in WT and Glut1 transgenic hearts (Fig. 3a,b). The heart was injured at P1, and EdU was injected intraperitoneally at P7 followed by cardiomyocyte isolation and flow cytometry analysis for Tnnt2, Mitotracker, and EdU signals. The percent EdU incorporation (mitotic index) of Tnnt2^{high} cardiomyocytes did not show significant difference between WT and Glut1 transgenic hearts or between sham and injured hearts (Fig. 3c, left). However, Tnnt2^{low} cardiomyocytes showed significantly higher mitotic activity in Glut1 transgenic cardiomyocytes than WT in both sham and injured hearts (12.9 ± 1.6 vs 3.6 ± 1.4, $p < 0.05$; Fig. 3c, right). This is consistent with the transcriptome data (Fig. 2), in which the genes related to the mitosis and cell cycle are significantly enriched in Tnnt2^{low} cells in Glut1 transgenic heart. Thus, data from transcriptomics and EdU incorporation assays suggest that Tnnt2^{low} subset, but not Tnnt2^{high} subset, of neonatal cardiomyocytes become mitotically potentiated in response to the increase in intracellular glucose.

Metabolomics analysis suggests an increase in glucose metabolites upon injury in Glut1 transgenic heart. Glucose is metabolized in multiple pathways including glycolysis, hexosamine biosynthesis pathway, and the pentose phosphate pathway (PPP). Having demonstrated that the increase in cardiac glucose uptake potentiates the regeneration of neonatal heart, we sought for its downstream mechanism. Metabolomics analysis of uninjured Glut1 transgenic hearts showed a significant increase in glucose metabolites including nucleotides (AMP and CMP; Fig. 4a, Supplementary Fig. 5a,b). Albeit strong overexpression of Glut1 protein and mRNA in the Glut1 transgenic hearts (Supplementary Fig. 1a,b), the intracellular glucose level was only mildly increased. However, glucose seems to be actively utilized upon injury in Glut1 hearts as evidenced by the significant increase in polyol pathway (sorbitol/mannitol, fructose) at P2 post-injury. Injury also caused the increase in the metabolites in the PPP in Glut1 transgenic hearts at P7 (Fig. 4a, Supplementary Fig. 5a,b).

In many species, cardiac glycogen content sharply decreases within 2 weeks after birth[22]. This was confirmed by our Periodic Acid Schiff (PAS) staining and quantitative measurement of glycogen content in WT hearts (Fig. 4b,c). Interestingly, Glut1 transgenic heart maintained significant level of glycogen accumulation after birth (0.39 ± 0.045 vs 0.0032 ± 0.00012 and 0.34 ± 0.019 vs 0.00033 ± 0.000035, $^{*}p < 0.05$ and $^{**}p < 0.01$; Fig. 4c), indicating that excess glucose is partly stored in the form of glycogen.

Inhibition of the nucleotide biosynthesis abrogates the regenerative advantage of Glut1 transgenic heart. Our previous report found that glucose promotes cardiomyocyte proliferation at the expense of cardiac maturation via the nucleotide biosynthesis during fetal development[10]. Although the levels of the nucleotides are not significantly higher in the Glut1 transgenic hearts post-injury, metabolomics data do not directly indicate the flow of each metabolites. To test whether nucleotide biosynthesis plays a central role in the glucose-induced cardiomyocyte regeneration, the neonatal hearts were injured in the presence of hydroxyurea (HU). HU is an inhibitor of ribonucleotide reductase (RNR), the rate-limiting enzyme of the nucleotide biosynthesis, that passes through the placenta when intraperitoneally injected to the pregnant mother[23]. 10 mg/kg of HU was intraperitoneally injected daily for 7 days starting 4 h prior to the cryoinjury at P1 until the EdU incorporation assay at P7 (Fig. 5a). HU blocked EdU incorporation in both Tnnt2^{low} and Tnnt2^{high} cardiomyocytes

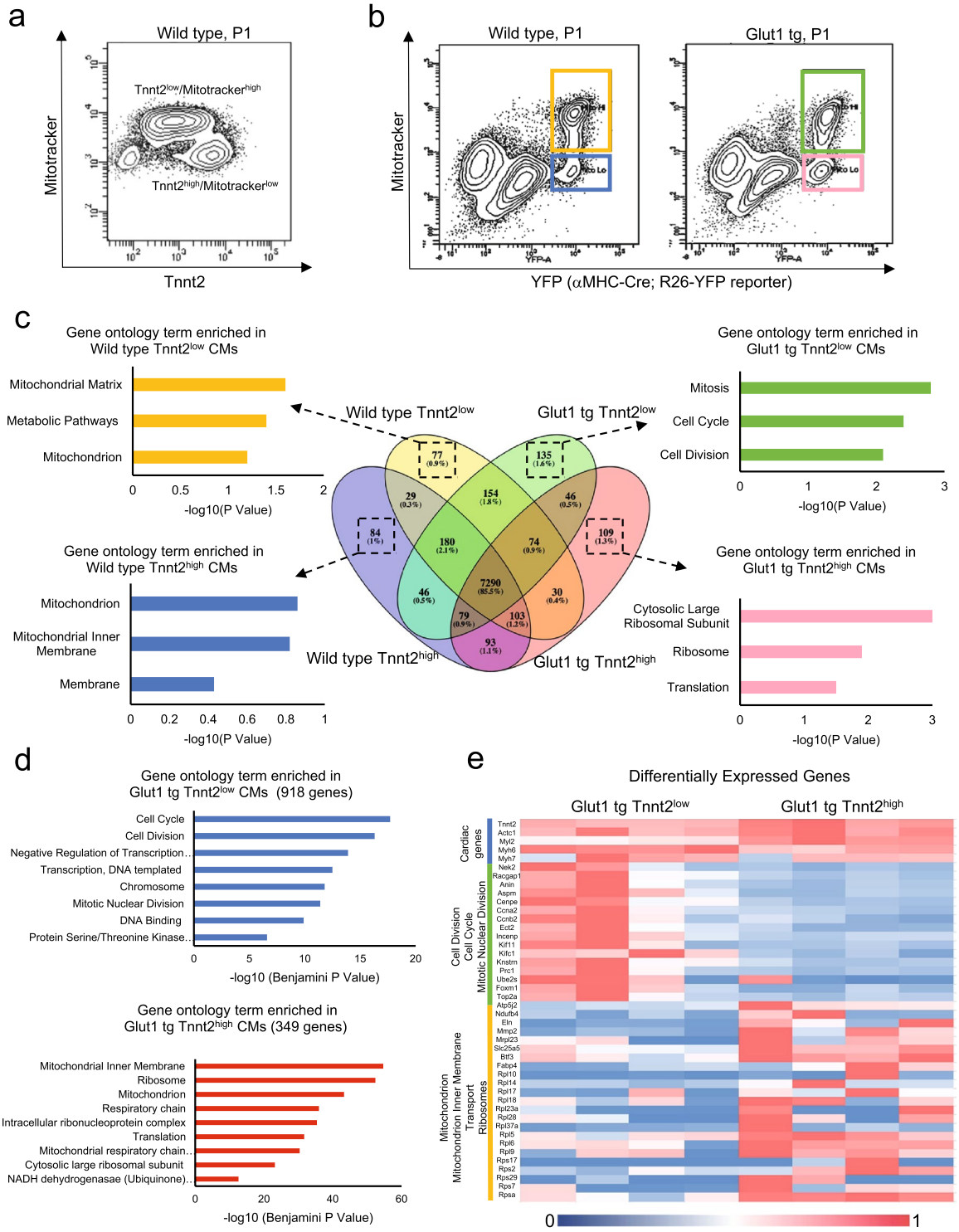

Figure 2. mRNA expression profile of Tnnt2^{high} and Tnnt2^{low} cardiomyocytes from Wild type and Glut1 transgenic hearts at P1. (**a**) Representative dot plot of flow cytometry analysis of P1 Wild type hearts for Tnnt2 (cardiac marker) and Mitotracker (mitochondrial contents). Note two populations of cardiomyocytes. (**b**) Flow cytometry analysis of P1 *aMHC-Cre ^{tg}; R26$^{+/YFP\ reporter}$* and *aMHC-hGLUT1 ^{tg}; aMHC-Cre ^{tg}; R26$^{+/YFP\ reporter}$* analysis for YFP (cardiac lineage) and Mitotracker (mitochondrial contents). Note two populations of cardiomyocytes. (**c**) Venn diagram of mRNA expressed in Tnnt2^{high} and Tnnt2^{low} cardiomyocytes from Wild type and Glut1 transgenic hearts. Bar graphs represent top three gene ontology (GO) term enriched in the genes uniquely expressed in each population. Although 4 populations are similar, G1 Tnnt2^{low} cardiomyocytes are enriched for the genes associated with mitosis, cell cycle, and cell division. (**d**) GO analysis of the genes upregulated in Glut1 tg Tnnt2^{low} vs Glut1 tg Tnnt2^{high}. (**e**) Heatmap of expression level of representative cardiac, cell cycle, and mitochondrial genes differentially expressed in Glut1 tg Tnnt2^{low} vs Glut1 tg Tnnt2^{high}.

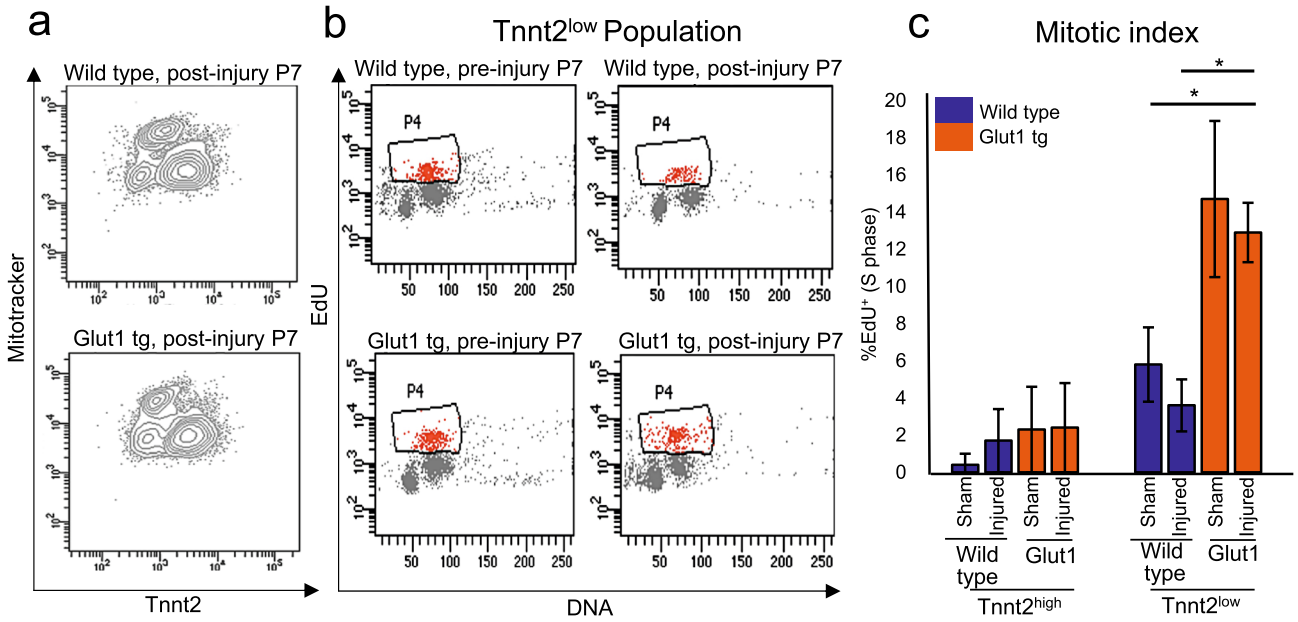

Figure 3. Tnnt2^{low} cardiomyocytes are mitotically activated by the increase in intracellular glucose. (**a**) Representative flow cytometry profile of the ventricular cardiomyocytes from P7 Wild type and Glut1 transgenic hearts stained with Tnnt2 and Mitotracker. (**b**) Representative flow cytometry plot of EdU incorporation assay of Tnnt2^{low} cardiomyocytes. Wild type and Glut1 transgenic mice were injected with EdU and the ventricular cardiomyocytes were isolated and analyzed by Tnnt2, Mitotracker, and EdU staining. (**c**) Mitotic index of Tnnt2^{high} and Tnnt2^{low} cardiomyocytes in Wild type and Glut1 transgenic heart with or without injury. n = 3–8. $^{*}p < 0.05$. $^{***}p < 0.001$. Note that Tnn2^{low} cardiomyocytes are more mitotic than Tnn2^{high} cardiomyocytes and that the mitotic activity of Tnnt2^{low} cardiomyocytes drastically increases in Glut1 transgenic background.

(Fig. 5b), and the number of Tnnt2^{low} cardiomyocytes was significantly reduced compared to the vehicle controls (Fig. 5c). Thus, Tnnt2^{low} cardiomyocytes contribute to cardiac regeneration in a glucose-dependent manner via the supply of nucleotides.

Discussion

In this study, we demonstrated that glucose metabolism is a determinant of regenerative capacity of the heart. By increasing basal intra-cardiomyocyte glucose uptake using transgenic mice that specifically overexpresses Glut1, we successfully enhanced the regenerative capacity of neonatal mouse hearts. We identified two distinct subpopulations of cardiomyocytes that have not been previously described; relatively mature (Tnnt2^{high}) and immature (Tnnt2^{low}) cardiomyocytes. Interestingly, the increase in the intracellular glucose promotes mitotic activity only in the Tnnt2^{low} subset of cardiomyocytes. Thus, Tnnt2^{low} subset of cardiomyocytes are the glucose-responders that proliferate in response to high glucose uptake upon heart injury, resulting in acceleration of heart regeneration.

Shortly after birth, the cardiomyocytes undergo terminal differentiation, and the response to the stress and extracellular signals changes. For example, Angiotensin II (Ang-II) or phenylephrine (PE) directly stimulates hypertrophy of the heart via the ERK/MAPK pathway at postnatal stages, while the same signals trigger hyperplasia during late gestational stages[24]. Our data suggest increased glucose metabolism potentiates the hyperplastic growth upon cardiac injury at neonatal stages in Glut1 transgenic heart. In adult heart, Glut1-overexpressing cardiomyocytes seem to respond to the pressure overload predominantly by hypertrophic growth[11]. However, it is unknown whether cardiomyocyte proliferation is simultaneously stimulated in the adult Glut1 transgenic hearts. Further investigation will determine whether glucose loading strategy may promote the regeneration of adult heart.

There is generally an inverse correlation between cell proliferation and differentiation during developmental stages[25]. In our previous study, we found that the nucleotide biosynthesis supported by the PPP is a key mechanism balancing cell proliferation and maturation during the physiological growth of cardiomyocytes. The balance between proliferation and maturation was successfully manipulated by addition of glucose or nucleotides (gain-of-function) and inhibition of the PPP and nucleotide biosynthesis (loss-of-function) in the in vitro settings[10]. The current study demonstrates that similar intervention may be effective during the neonatal stages to accelerate regeneration. Indeed, metabolic profiling of neonate hearts revealed that glucose is actively utilized in the context of cryoinjury, evidenced by the marked accumulation of polyol pathway intermediates. The influence of metabolic activity, driven by glucose utilization, on regulating cardiac regeneration was probed further through pharmacological intervention. The regenerative advantage of Glut1 transgenic heart was abrogated by the inhibition of RNR, the key enzyme of nucleotide biosynthesis pathway, by HU, further re-emphasizing the importance of the nucleotides in regulating cardiomyocyte proliferation and regeneration upon injury.

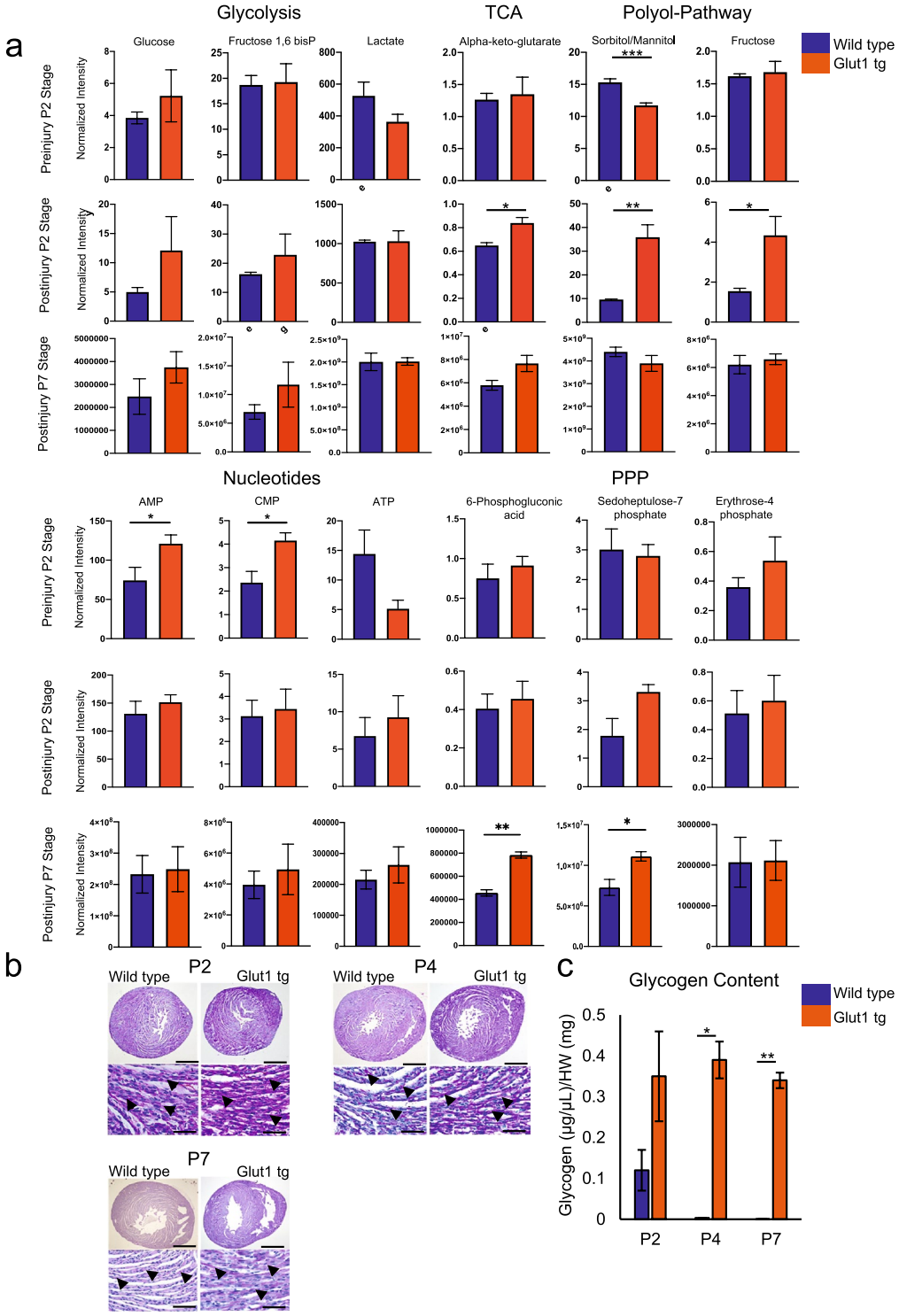

Figure 4. Metabolomics analysis of Glut1 transgenic hearts. (**a**) Metabolomics analysis of Glut1 transgenic hearts and wild type litters at P2 pre-injury and post-injury and P7 post-injury. At P2 stage, overall, the metabolic profile shows no drastic difference at the basal level, but glucose utility increases upon injury as represented by the increase in the metabolites in polyol pathway and glucose. At P7 stage, the metabolic profile showed a statistical differences of intermediates in the Pentose Phosphate Pathway. n = 3 wild type, n = 6 Glut1 tg hearts. *$p < 0.05$. **$p < 0.01$. (**b**) Histological analysis of glycogen storage of Glut1 transgenic hearts and its controls from wild type litters at P2, P4 and P7 by Periodic Acid Staining. Representative images of 3 samples in each group. Scale bar = 200 µm and 20 µm respectively. (**c**) Glycogen quantification by colorimetric assay kit at P2, P4 and P7 stage. n = 3 per group. *$p < 0.05$. **$p < 0.01$. Note the increased intracellular glycogen storage in Glut1 transgenic hearts.

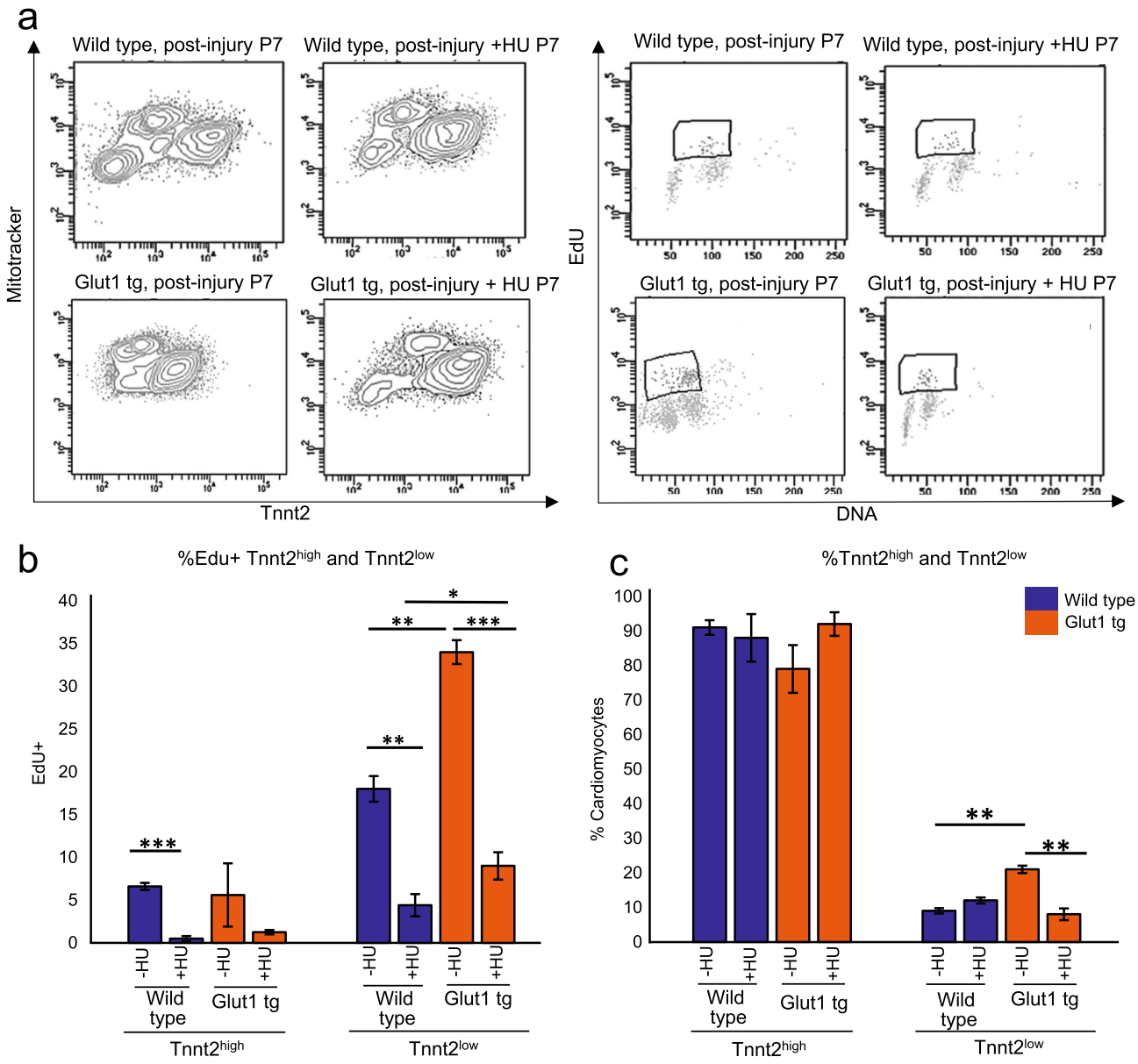

Figure 5. Impact of hydroxyurea on the proliferation of Tnnt2^{low} cardiomyocytes. (**a**) Representative contour plots (left) for Tnnt2 and Mitotracker and dot plots (right) for EdU and DNA content by flow cytometry analysis at P7. Wild type and Glut1 transgenic hearts were cryoinjured at P1 and treated with daily injection of HU or vehicle until the analysis at P7. (**b**) Quantification of %EdU positive cells in Tnnt2^{high} and Tnnt2^{low} cardiomyocytes in wild type and Glut1 transgenic hearts with or without HU treatment. Note that both Tnnt2^{high} and Tnnt2^{low} cardiomyocytes respond to HU treatment but that EdU incorporation of Tnnt2^{low} cardiomyocytes was drastically decreased by HU treatment. n = 4. ***$p < 0.01$. (**c**) Quantification of the Tnnt2^{high} and Tnnt2^{low} fractions of cardiomyocytes in wild type and Glut1 transgenic hearts with or without HU treatment. While Tnnt2^{high} or Tnnt2^{low} fractions was not influenced by HU in wild type heart, HU treatment significantly decreased the percentage of Tnnt2^{low} cardiomyocytes in Glut1 transgenic hearts. n = 4. **$p < 0.01$. ***$p < 0.001$.

Cells display distinct metabolic profiles depending on their differentiation stage[26–28]. The fuel type of cells serves not merely as a source of energy but also as a regulator of self-renewal and differentiation of stem or progenitor cells[29–32]. Among such metabolic factors, environmental glucose is one of the fundamental nutrients for the cells and is a significant contributor to heart formation. However, despite the established association between hyperglycemia and the heart malformation, little is known about how glucose impacts cardiomyocyte formation and re-formation[33–35]. Glucose induces cardiomyocyte proliferation at the sacrifice of its maturity via the pentose phosphate pathway and nucleotide biosynthesis during physiological heart formation[10]. The current study is the first to demonstrate that glucose metabolism is a critical determinant of cardiac regenerative capacity through the nucleotide biosynthesis in vivo. The non-genetic factors and genetic regulators mutually reinforce each other to establish a robust cardiac differentiation program. Metabolic environment of the cells is, on one hand,

determined by the genetic program of cells. On the other hand, the genetic program of the cells is dependent on the metabolic environment. Understanding how the genetic program and metabolic factors crosstalk during physiological and pathological cardiogenesis will be an important theme that requires further investigation.

Materials and methods

Mouse maintenance and cryoinjury of neonatal mouse hearts. Animals were housed at the University of California Los Angeles (UCLA) animal facility. WT and Glut1 transgenic mice (males and females) were maintained on the ICR/CD-1 strain background according to the Guide for the Care and Use of Laboratory Animals published by the US National Institute of Health (NIH Publication No. 85-23, revised 1996). Housing and experiments were performed according to the Institutional Approval for Appropriate Care and Use of Laboratory Animals by the UCLA Institutional Animal Care and Use Committee (Protocol # 2008-143-31). Some WT ICR/CD-1 mom and pups were ordered from Charles River Laboratories, MA and housed at the UCLA animal facility. The study was carried out in compliance with the ARRIVE guidelines. Surgical procedures were performed as previously described[36] with some modifications in order to optimize the time of injury to the apex of the left ventricle while creating a non-transmural injury as well as optimizing the time for adequate anesthesia and decreasing post-surgical mortality of the pups. Briefly, 1-day old neonatal mice were anesthetized under hypothermic conditions. Left lateral thoracotomies at the 5th intercostal space were performed and hearts were exposed through an incision at intercostal space 5–6. As soon as the incision was made, a 1 mm metal probe was chilled in liquid nitrogen for 15–30 s. After heart exposure, the pre-chilled probe was placed on the apex of the left ventricle for 1 s. Sham operated hearts were also exposed for 1 s but no injury was done. The thoracic wall incision was closed with a 7–0 Prolene suture (8701H, Ethicon, Somerville, NJ USA) using a figure of eight suture technique. The skin was closed by topical tissue adhesive (Gluture, Abbott Laboratories, IL, USA). After surgery, pups were placed immediately in a warm water bed and allowed to full recovery for at least 15 min prior to putting pups back in the cage with mom. The survival rate was around 90%. Body weights were measured (grams) using a weight scale prior to each cryosurgery and plasma glucose levels were measured by using a ONE TOUCH Glucose Monitor using blood samples obtained by tail bleeding.

Tissue collection and histological analysis. To collect hearts at different time points, mice were put under general anesthesia with 99.9% isoflurane in an inhalation chamber followed by cervical dislocation. Body weights were measured prior to collection of hearts. After collection of hearts, they were weighed using an analytical balance weight scale. Hearts were dissected and cleaned prior to weighting. Pictures were taken for each heart in order to analyze phenotypic differences between the transgenic Glut1 hearts and the WT hearts. Hearts were embedded in paraffin and sectioned transversely from the apex to the base at 7 μm. Paraffin sections from hearts at 1, 2, 3 and 6 weeks after surgery were stained with Hematoxylin and Eosin according to standard protocols to evaluate the extent of injury. The heart sections were also stained with Picrosirius Red Staining to order to determine the extent of collagen deposition. After deparaffinization in Xylene, the sections were washed with ethanol and PBS, incubated with picrosirius red solution for 1 h at room temperature, and then rinsed quickly with acetic acid and ethanol. Stained sections were dehydrated with ethanol and xylene and mounted. In Picrosirius Red stained sections, the scar tissue is stained red and muscle tissue appears yellow. For immunostaining, sections were incubated with the following primary antibodies: cardiac TnnT2 (Sigma Cat# HPA015774 1:1000 rabbit), Proliferating Cell Nuclear Antigen (Vector laboratories PCNA Cat#VP-P980), and PECAM (eBioscience Cat# 13-0311) for 1 h. Heart sections were also stained with Periodic Acid Schiff stain kit (Abcam) at post-natal stage 2 days in order to determine the glycogen content within these hearts. Glycogen stained magenta in color while nuclei stained blue.

Flow cytometry. Hydroxyurea (HU) and Edu were injected intraperitoneally. HU injections were performed 4 h prior to cryoinjury and daily for 7 days. Edu was injected 4 h prior to tissue harvest, hearts were dissociated to single cells at P7 as previously described[10,37]. The cells were stained for Mitotracker Orange CMTMRos (ThermoFisher), and further fixed and strained with Tnnt2 antibody (rabbit, 1:200, Sigma-Aldrich) and ClickIT EdU kit. Alexa488-conjugated anti-rabbit IgG antibody (ThermoFisher) was used for secondary antibody for TnnT2. Stained cells were analyzed by a flow cytometer (LSRII, BD Biosciences). Data analysis was performed using FACSDiva (BD Biosciences).

RNA-Seq and data analyses. Tnnt2^{high} and Tnnt2^{low} cardiomyocytes from *αMHC-Cre^{tg}; R26$^{+/YFP\ reporter}$* and *αMHC-hGLUT1^{tg}; αMHC-Cre^{tg}; R26$^{+/YFP\ reporter}$* were sorted using Mitotracker and YFP and their RNAs were extracted using RNeasy kit (QIAGEN). mRNA library was prepared with the Illumina HiSeq mRNA kit (Illumina, RS-122-2001), according to manufacturer's instructions. Final libraries were sequenced with single-end reads of 50 bp on Illumina sequencing platforms HiSeq 3000 (Illumina, San Diego, CA); raw sequencing reads were assessed for quality using FastQC (www.bioinformatics.babraham.ac.uk/projects/fastqc), then low-quality bases with a Phred quality value lower than 20 were trimmed off the read ends. The RNA Sequencing reads were mapped to mouse genome assembly UCSC mm10 using the HISAT2 with default settings[38]. UCSC annotation release mm10 was used to identify genes for feature counting. Read counts for genes were determined as counts mapped to the union of all exons for all transcript isoforms of a given gene using HTSeq[39]. Differential expression analysis and generation of the corresponding data plots were performed using DESeq2 using default settings, except that the alpha (FDR) threshold was set to 0.05[40].

^{18}F-FDG measurement by autoradiography. Autoradiography was conducted as we described[41] except that mouse pups were injected with ^{18}F-FDG (3.33 MBq; UCLA Ahmanson Biomedical Cyclotron Facility) and

hearts were removed and sliced at 7 μm of thickness for analysis. Heart ^{18}F-FDG accumulation was quantified using Fujifilm Multi Gauge v.3.0 software and the signal was normalized to the amount of probe injected for each mouse pup.

Intracellular metabolite extraction and analysis. Neonatal hearts were excised and weighed. Hearts were submerged in 500 μl of extraction solution (80% methanol/10 μM trifluoromethanosulfanate) contained in 2 mL tubes containing 1.4 mm ceramic beads. Tubes were placed in a Bead Mill 4 (Fisher brand) to homogenize tissue for 6 min (speed: 6 m/s). Homogenates were transferred to clean tubes and centrifuged at 4 °C for 10 min at 17,000*g*. For every sample, a supernatant volume that is equivalent to 5 mg of total heart tissue was transferred to a glass vial. Samples in glass vials were dried under an EZ-2Elite evaporator. Metabolites were resuspended in 100 μl 50% acetonitrile (ACN). The analysis was performed on a Q Exactive (Thermo Scientific) in polarity-switching mode with positive voltage 3.5 kV and negative voltage 3.5 kV. The mass spectrometer was coupled to an Vanquish (Thermo Scientific) UHPLC system. Mobile phase A was 5 mM NH_4Ac, pH 9.9, B was ACN. Separation was achieved on a Luna 3 mm NH_2 100 A (150 × 2.0 mm) (Phenomenex) column kept at a temperature of 40 °C. Injection volume was 10 μl, flow was 200 μl/min, and the gradient ran from 15% A to 95% A in 18 min, followed by an isocratic step for 9 min and re-equilibration for 7 min. Metabolites were detected and quantified as the area under the curve based on retention time and accurate mass (≤ 15 p.p.m.) using MZMine 2.0.

Glycogen content determination. Cardiac glycogen levels were quantified using Glycogen Assay Kit (Colorimetric/Fluorometric) (ab65620). Neonatal hearts at P2, P4 and P7 were excised and weighted. Tissues were homogenized in ddH_2O and boil for 10 min. Samples were centrifuged and the supernatant was collected in a new tube. Glycogen standard (0.2 mg/ml) was used to prepare a standard curve dilution ranging from 0 to 2 μg/well. Reaction wells were set up per assay protocol. Serial dilutions were used and (1:16 dilution) was found to be the optimal dilution for our samples. All standard and sample wells were set up to have duplicate readings. Glucose was analyzed by colorimetric reading immediately after incubation with enzyme mix using a microplate reader at optical density (OD) of 570 nm.

Transthoracic echocardiography. Murine transthoracic 2D M-mode and Doppler imaging echocardiography was conducted using a VisualSonics Vevo 2100 ultrasound system and a 30-MHz probe. The mice were sedated using isoflurane inhalation (1.5–2%) and were spontaneously breathing during the procedure. Mice chest fur was removed using depilatory cream. The heart was imaged in the two-dimensional parasternal long and short-axis view, and an M-mode echocardiogram of the mid-ventricle was recorded at the level of the papillary muscles. Heart rate, end-diastolic and end-systolic internal dimensions of the left ventricle were measured from the M-mode image. LV ejection fraction was used as an index of cardiac function and fractional shortening was used as an index of cardiac contractility.

Quantification and statistics. Data are presented as mean ± SEM. Comparison between the two groups was done by the two tailed Student's T test. $^{*}p < 0.05$ and $^{**}p < 0.01$ were considered statistically significant. Quantification of angiogenesis and scar size as a ratio of scar area to the left ventricular area was conducted manually by using Image J software by one observer, however the observer was not blinded to the experimental groups.

Received: 8 January 2020; Accepted: 9 April 2021
Published online: 21 April 2021

References

1. Porrello, E. R. *et al.* Transient regenerative potential of the neonatal mouse heart. *Science (New York, N.Y.)* **331**, 1078–1080 (2011).
2. Mollova, M. *et al.* Cardiomyocyte proliferation contributes to heart growth in young humans. *Proc. Natl. Acad. Sci. U.S.A.* **110**, 1446–1451 (2013).
3. Bergmann, O. *et al.* Dynamics of cell generation and turnover in the human heart. *Cell* **161**, 1566–1575 (2015).
4. Bergmann, O. *et al.* Evidence for cardiomyocyte renewal in humans. *Science (New York, N.Y.)* **324**, 98–102 (2009).
5. Mahmoud, A. I. *et al.* Meis1 regulates postnatal cardiomyocyte cell cycle arrest. *Nature* **497**, 249–253 (2013).
6. Soonpaa, M. H., Kim, K. K., Pajak, L., Franklin, M. & Field, L. J. Cardiomyocyte DNA synthesis and binucleation during murine development. *Am. J. Physiol.* **271**, H2183-2189 (1996).
7. Kuhn, B. *et al.* Periostin induces proliferation of differentiated cardiomyocytes and promotes cardiac repair. *Nat. Med.* **13**, 962–969 (2007).
8. Patterson, M. *et al.* Frequency of mononuclear diploid cardiomyocytes underlies natural variation in heart regeneration. *Nat. Genet.* **49**, 1346–1353 (2017).
9. Murashige, D. *et al.* Comprehensive quantification of fuel use by the failing and nonfailing human heart. *Science* **370**, 364–368 (2020).
10. Nakano, H. *et al.* Glucose inhibits cardiac muscle maturation through nucleotide biosynthesis. *Elife* **6**, e29330 (2017).
11. Liao, R. *et al.* Cardiac-specific overexpression of GLUT1 prevents the development of heart failure attributable to pressure overload in mice. *Circulation* **106**, 2125–2131 (2002).
12. Paternostro, G., Clarke, K., Heath, J., Seymour, A. M. & Radda, G. K. Decreased GLUT-4 mRNA content and insulin-sensitive deoxyglucose uptake show insulin resistance in the hypertensive rat heart. *Cardiovasc. Res.* **30**, 205–211 (1995).
13. Abel, E. D. *et al.* Cardiac hypertrophy with preserved contractile function after selective deletion of GLUT4 from the heart. *J. Clin. Investig.* **104**, 1703–1714 (1999).
14. Montessuit, C. & Thorburn, A. Transcriptional activation of the glucose transporter GLUT1 in ventricular cardiac myocytes by hypertrophic agonists. *J. Biol. Chem.* **274**, 9006–9012 (1999).

15. Gamba, L., Harrison, M. & Lien, C. L. Cardiac regeneration in model organisms. *Curr. Treat. Opt. Cardiovasc. Med.* **16**, 288 (2014).
16. Darehzereshki, A. *et al.* Differential regenerative capacity of neonatal mouse hearts after cryoinjury. *Dev. Biol.* **399**, 91–99 (2015).
17. Schneider, C. A., Rasband, W. S. & Eliceiri, K. W. NIH Image to ImageJ: 25 years of image analysis. *Nat. Methods* **9**, 671–675 (2012).
18. Porrello, E. R. *et al.* Regulation of neonatal and adult mammalian heart regeneration by the miR-15 family. *Proc. Natl. Acad. Sci. U.S.A.* **110**, 187–192 (2013).
19. Doherty, E. & Perl, A. Measurement of mitochondrial mass by flow cytometry during oxidative stress. *React. Oxyg. Species (Apex)* **4**, 275–283 (2017).
20. de Carvalho, A. *et al.* Early postnatal cardiomyocyte proliferation requires high oxidative energy metabolism. *Sci. Rep.* **7**, 15434 (2017).
21. de Almeida, M. J., Luchsinger, L. L., Corrigan, D. J., Williams, L. J. & Snoeck, H. W. Dye-independent methods reveal elevated mitochondrial mass in hematopoietic stem cells. *Cell Stem Cell* **21**, 725–729 (2017).
22. Shelley, H. J. Glycogen reserves and their changes at birth and in anoxia. *Br. Med. Bull.* **17**, 137–143 (1961).
23. Campion, S. N. *et al.* Sensitive windows of skeletal development in rabbits determined by hydroxyurea exposure at different times throughout gestation. *Birth Defects Res. B Dev. Reprod. Toxicol.* **95**, 238–249 (2012).
24. Sundgren, N. C., Giraud, G. D., Stork, P. J., Maylie, J. G. & Thornburg, K. L. Angiotensin II stimulates hyperplasia but not hypertrophy in immature ovine cardiomyocytes. *J. Physiol.* **548**, 881–891 (2003).
25. Ruijtenberg, S. & van den Heuvel, S. Coordinating cell proliferation and differentiation: Antagonism between cell cycle regulators and cell type-specific gene expression. *Cell Cycle* **15**, 196–212 (2016).
26. Carey, B. W., Finley, L. W., Cross, J. R., Allis, C. D. & Thompson, C. B. Intracellular alpha-ketoglutarate maintains the pluripotency of embryonic stem cells. *Nature* **518**, 413–416 (2015).
27. Tohyama, S. *et al.* Distinct metabolic flow enables large-scale purification of mouse and human pluripotent stem cell-derived cardiomyocytes. *Cell Stem Cell* **12**, 127–137 (2013).
28. Wang, J. *et al.* Dependence of mouse embryonic stem cells on threonine catabolism. *Science (New York, N.Y.)* **325**, 435–439 (2009).
29. Harris, J. M. *et al.* Glucose metabolism impacts the spatiotemporal onset and magnitude of HSC induction in vivo. *Blood* **121**, 2483–2493 (2013).
30. Oburoglu, L. *et al.* Glucose and glutamine metabolism regulate human hematopoietic stem cell lineage specification. *Cell Stem Cell* **15**, 169–184 (2014).
31. Shiraki, N. *et al.* Methionine metabolism regulates maintenance and differentiation of human pluripotent stem cells. *Cell Metab.* **19**, 780–794 (2014).
32. Shyh-Chang, N. *et al.* Influence of threonine metabolism on S-adenosylmethionine and histone methylation. *Science (New York, N.Y.)* **339**, 222–226 (2013).
33. Centers for Disease, C. Perinatal mortality and congenital malformations in infants born to women with insulin-dependent diabetes mellitus—nited States, Canada, and Europe, 1940–1988. *MMWR Morb. Mortal Wkly. Rep.* **39**, 363–365 (1990).
34. Yogev, Y. & Visser, G. H. Obesity, gestational diabetes and pregnancy outcome. *Semin. Fetal Neonatal Med.* **14**, 77–84 (2009).
35. Simeone, R. M. *et al.* Diabetes and congenital heart defects: A systematic review, meta-analysis, and modeling project. *Am. J. Prev. Med.* **48**, 195–204 (2015).
36. Polizzotti, B. D., Ganapathy, B., Haubner, B. J., Penninger, J. M. & Kuhn, B. A cryoinjury model in neonatal mice for cardiac translational and regeneration research. *Nat. Protoc.* **11**, 542–552 (2016).
37. Nakashima, Y. *et al.* Nkx2-5 suppresses the proliferation of atrial myocytes and conduction system. *Circ. Res.* **114**, 1103–1113 (2014).
38. Kim, D., Langmead, B. & Salzberg, S. L. HISAT: A fast spliced aligner with low memory requirements. *Nat. Methods* **12**, 357–360 (2015).
39. Anders, S., Pyl, P. T. & Huber, W. HTSeq—A Python framework to work with high-throughput sequencing data. *Bioinformatics* **31**, 166–169 (2015).
40. Love, M. I., Huber, W. & Anders, S. Moderated estimation of fold change and dispersion for RNA-seq data with DESeq2. *Genome Biol.* **15**, 550 (2014).
41. Shu, C. J. *et al.* Quantitative PET reporter gene imaging of CD8+ T cells specific for a melanoma-expressed self-antigen. *Int. Immunol.* **21**, 155–165 (2009).

Acknowledgements

Authors thank technical support from Dr. Morizono (AIDS institute, UCLA) and BSCRC FACS core. Authors are also grateful to Dr. Sherin Devaskar, Dr. Marlin Touma, and Dr. Josephine Enciso for helpful comments. This study was supported by NIH HL142801 to A.N, UCLA David Geffen School of Medicine (DGSOM) Seed Grant to A.N. and H.C., NIH HL130172 to C.L.L., UCLA Eli and Edythe Broad Center of Regenerative Medicine and Stem Cell Research (BSCRC) Training Grant and Children's Discovery and Innovation (CDI) Grant to V.M.F.

Author contributions

The project was conceptualized and designed by V.M.F., P.C., R.T., H.C., H.N., and A.N. The experiments were performed by V.M.F., I.F., B.Y.C., C.A.P., B.S., and H.N., and the data were analyzed by V.M.F., P.C., R.T., C.L., M.P., H.C., H.N. and A.N. The manuscript was written by V.M.F. and A.N. with the input from all the co-authors.

Competing interests

The authors declare no competing interests.

Additional information

Supplementary Information The online version contains supplementary material available at https://doi.org/10.1038/s41598-021-88159-x.

Correspondence and requests for materials should be addressed to A.N.

Reprints and permissions information is available at www.nature.com/reprints.

Publisher's note Springer Nature remains neutral with regard to jurisdictional claims in published maps and institutional affiliations.